Journal of Colloid and Interface Science 483 (2016) 41–48

Contents lists available at ScienceDirect

Journal of Colloid and Interface Science

journal homepage: www.elsevier.com/locate/jcis

Regular Article

Liquid crystal physical gel formed by cholesteryl stearate for light scattering display material

W.L. Leaw [a], C.R. Mamat [a,*], S. Triwahyono [a], A.A. Jalil [b,c], N. Bidin [d]

[a] Department of Chemistry, Faculty of Science, Universiti Teknologi Malaysia, 81310 UTM Johor Bahru, Johor, Malaysia
[b] Department of Chemical Engineering, Faculty of Chemical and Energy Engineering, Universiti Teknologi Malaysia, 81310 UTM Johor Bahru, Johor, Malaysia
[c] Centre of Hydrogen Energy, Institute of Future Energy, Universiti Teknologi Malaysia, 81310 UTM Johor Bahru, Johor, Malaysia
[d] Department of Physics, Faculty of Science, Universiti Teknologi Malaysia, 81310 UTM Johor Bahru, Johor, Malaysia

GRAPHICAL ABSTRACT

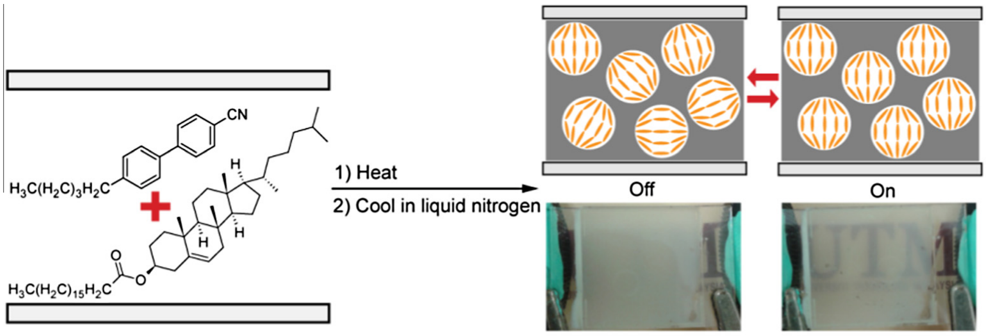

Cholesteryl stearate gelled 5CB for light scattering mode display

ARTICLE INFO

Article history:
Received 13 June 2016
Revised 8 August 2016
Accepted 10 August 2016
Available online 10 August 2016

Keywords:
Liquid crystal physical gel
Cholesteryl stearate
5CB
Light scattering

ABSTRACT

A liquid crystal physical gel was prepared by the self-assembly of cholesteryl stearate in a nematic liquid crystal, 4-cyano-4′-pentylbiphenyl. The electro-optical properties were tuned by varying the gelator concentration and the gelation conditions. Polarized optical microscopy revealed that cholesteric cholesteryl stearate induced chiral nematic phase in 4-cyano-4′-pentylbiphenyl during the gelation process. As a result, a plate-like gel structure consisting of spherical micropores was formed, as observed by scanning electron microscopy. Electron spin resonance spectroscopy showed that the liquid crystal director orientations in these macrophase-separated structures were massively randomised. For these reasons, the liquid crystal physical gel generated a strong light scattering effect. For 48.0 wt% cholesteryl stearate gelled 4-cyano-4′-pentylbiphenyl, the turbid appearance could be switched to a transparent state using a 5.0 V alternating current. The response time was about 3.7 μs. This liquid crystal physical gel has potential for use in light scattering electro-optical displays.

1. Introduction

Polymer-dispersed liquid crystals (PDLCs) are composed of micro-sized liquid crystal domains embedded in a continuous polymer matrix. This is an important class of materials for optoelectronic applications. Conventional PDLCs may have either a Swiss cheese or polymer ball-type morphology [1]. Basically, a mismatch in the refractive index between the liquid crystal and the polymer matrix produces a turbid appearance. Upon application of an applied voltage, the liquid crystal molecules are realigned

---

* Corresponding author.
E-mail address: che@kimia.fs.utm.my (C.R. Mamat).

http://dx.doi.org/10.1016/j.jcis.2016.08.020
0021-9797/

such that the higher relative permittivity of the liquid crystal is parallel with the electric field. Thus, the index of refraction of the liquid crystal becomes closely matched to that of the polymer matrix and thus the turbid appearance is switched to a transparent state [2]. Due to their simple design and manufacturing, PDLCs have been widely studied for large area displays, switchable windows, holographic film and other applications [3]. However, there are several practical problems such as high threshold voltage, low contrast ratio and slow response time. Most importantly, PDLCs are thermally irreversible, and reprocessing is impossible.

Thermal-reversible gel was then been invented by the self-assembly of a low molecular mass gelator in a liquid crystal medium via non-covalent interactions [4]. This material is called a liquid crystal physical gel. Liquid crystal physical gels based on room temperature nematic liquid crystals can be applied on both twisted nematic and light scattering mode displays. For light scattering mode, liquid crystal physical gels can be switched between the turbid and transparent state in the same way as PDLCs. Conventionally, a light scattering type liquid crystal physical gel is prepared using a gelator that has a gelation temperature (T_g) higher than the isotropic-nematic transition temperature (T_{IN}) of the nematic host [5]. When gelation happens in the isotropic medium of the liquid crystal, randomly dispersed fibrous networks are formed. Liquid crystal directors are misaligned depending on the morphology of the voids created by the fibrous network, and thus a light scattering effect is generated. Several reported gelators are the derivatives of an oligo (amino acid), 4,4′-diaminodiphenylmethane, sorbitol or other compounds. To the best of our knowledge, all the reported gelators form only fibrous networks, and the microphase-separated structures are always non-uniform in shape. Therefore, ideally spherical liquid crystal droplets are rarely formed.

In this study, we aimed to produce liquid crystal physical gel with a plate-like structure instead of a fibrous form. To do this, we gelled nematic 5CB using a cholesteric gelator, namely cholesteryl stearate (G1). The chemical structures of cholesteryl stearate and 4-cyano-4′-pentylbiphenyl are shown in Fig. 1. We hypothesised that cholesteryl stearate, which possesses a cholesteric mesomorphic phase, could induce nematic 5CB to possess a chiral phase during the gelation process due to its molecular chirality. Hence, the gel structure formed is different from that formed in an isotropic medium. Notably, cholesteryl stearate successfully gelled 5CB into piles of plate-like stacking aggregates. The macrophase-separated structures were prepared at different cooling temperatures and the relative electro-optical responses were therefore examined.

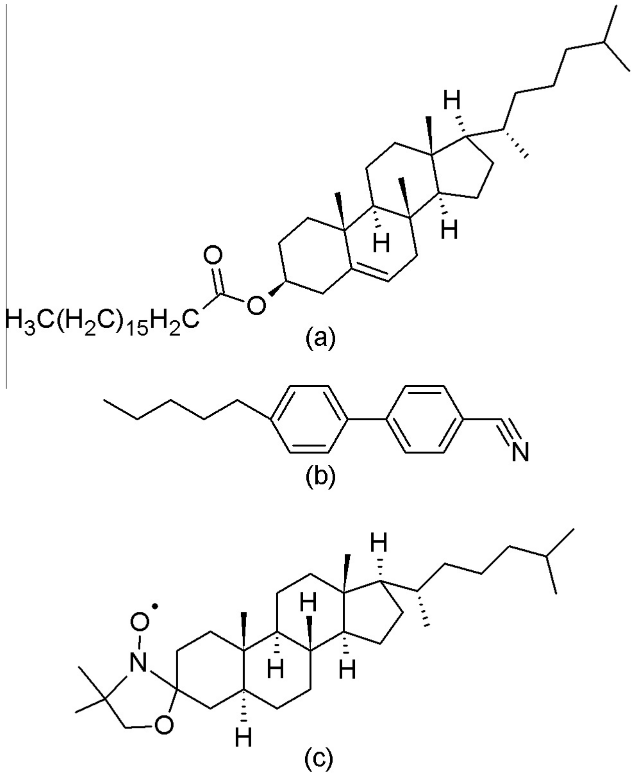

Fig. 1. Chemical structure of (a) cholesteryl stearate gelator (G1), (b) 4-cyano-4′-pentylbiphenyl (5CB) and (c) 3β-DOXYL-5α-cholestane free radical.

2. Experimental

2.1. Liquid crystal physical gel preparation

The minimum gelator concentration of G1 was determined by the tube inversion method [6]. First, suitable amount of G1 was mixed into 5CB followed by heating to 120 °C under continuous stirring to achieve isotropic state. The solution was cooled to room temperature and kept for several hours to ensure complete gelation. The glass tube containing G1/5CB composite was inverted upside down while the flow of sample was checked visually. If no fluid ran down the wall of glass tube upon inversion, gelation was confirmed.

For optical cell preparation, G1 and 5CB mixture was heated to isotropic state and was then flow-filled into non-rubbed, indium tin oxide (ITO)-coated cell (purchased from Instec, Inc.). The cell gap is 19.5 μm. The kinetic of the gelation process is known to affect the morphology of the aggregates. Fast cooling always produces finely dispersed networks of small aggregates. In this study, the optical cell containing isotropic mixture was instantly dipped into liquid nitrogen to perform rapid cooling.

2.2. Liquid crystal physical gel characterizations

The alignment and distribution of gel networks in liquid crystal were observed using optical microscope (AmScope-ME520TA) equipped with polarizers. For scanning electron microscopy (SEM) observation of the morphology of the gel network, the optical cell containing liquid crystal physical gel was extracted using hexane:ethyl acetate (1:10) for 3 h. The optical cell was carefully disassembled and dried xerogel on the glass surface was sputter-coated with platinum before analysis.

The electro-optical response of the liquid crystal physical gel was studied by measuring the transmission as a function of applied voltage using experimental setup as shown in Fig. 2. The optical cell was placed between He-Ne laser and photodiode (Thorlabs, PDA36A-EC) that connected to oscilloscope (Tektronix, TDS 3052C). He-Ne laser (632.8 nm) was used as an incident light source. Frequency of AC electric field was set to 300 Hz. The light intensity of optical cell filled with toluene was set as maximum light intensity. The threshold voltage (V_{10}) and saturation voltage (V_{90}) were defined as the applied voltage to obtain 10% and 90% of the maximum transmittance of each sample, respectively. The contrast ratio (CR) was calculated as the ratio of maximum transmittance at 100 V to minimum transmittance at 0 V. The rise time and decay time were measured as the time to reach 90% and drop back to 10% of the maximum transmittance, respectively. All measurements were performed at room temperature.

Variable-temperature FT-IR measurements were performed on IRTracer-100 spectrometer equipped with a hot stage [7]. Temperatures were set as 27, 40 and 60 °C. Electron spin resonance spectra were recorded using JEOL JES-FA 100 ESR spectrometer to investigate the impact of gelator network to the director orientation of

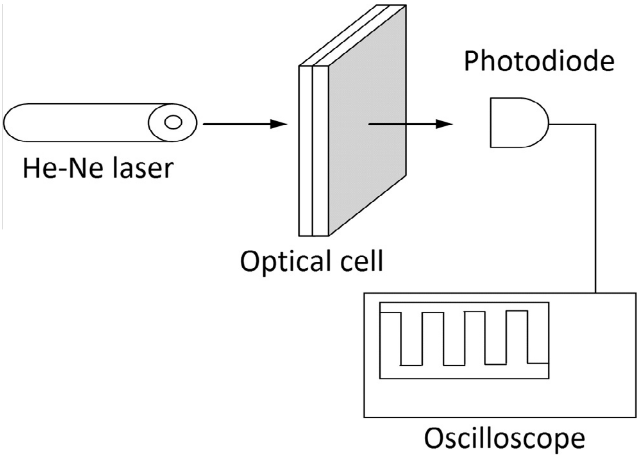

Fig. 2. Setup for electro-optical measurement.

liquid crystals [8–11]. 3β-DOXYL-5α-cholestane free radical as shown in Fig. 1 was used as spin probe due to the diamagnetic properties of liquid crystal physical gels. For sample preparation, spin probe in dichloromethane (10^{-4} M) was placed into sample tube followed by removal of solvent. Mixture of liquid crystal and gelator was placed into the same sample tube. Finally, mixture was heated using hot air gun followed by cooling.

3. Results and discussion

3.1. Gelation of liquid crystal physical gel

The minimum concentration of G1 to gel 5CB was determined by the tube inversion method. 5CB was successfully gelled by 6.0 wt% of G1, taking several hours at room temperature. The composite remained static when the glass tube was inverted upside down at room temperature as shown in Fig. 3. Theoretically, gelation undergoes three stages, namely the recognition of molecules, aggregation and the interconnection of aggregates; these stages are highly dependent on the interaction between the gelator and the host medium. The slow gelation process is therefore caused by the high solubility of G1 in mesogenic medium. Consequently, the gelator has a low tendency to solidify into aggregates. This phenomenon was also observed by Wang et al. when they used a mesogenic azobenzene derivative to gel a liquid crystal [12].

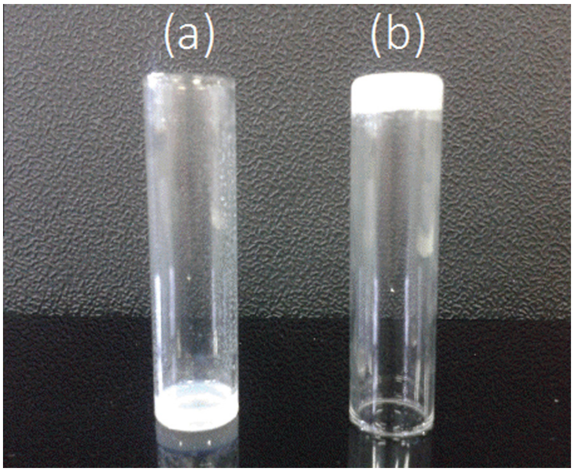

Fig. 3. Photograph of 6.0 wt% G1/5CB at (a) isotropic state and (b) gel state.

Optical cells with liquid crystal physical gels at the concentrations of 6.0, 12.0, 24.0 and 48.0 wt% were prepared. During preparation, an optical cell containing the isotropic mixture was observed using POM while the sample was undergoing the gelation process. Fig. 4 shows the phase transition during the gelation process of 6.0 wt% G1/5CB. When the sample was heated to the isotropic state, the POM images showed only a dark background since incident light could not be rotated by the isotropic medium across the crossed polarisers. Surprisingly, the fingerprint texture of the cholesteric phase was observed throughout the sample before gelation [13–15]. The fingerprint texture of the cholesteric phase also appeared during the gelation process of 12.0, 24.0 and 48.0 wt% G1/5CB. The chirality of the cholesteryl stearate transferred the nematic phase of 5CB to the cholesteric phase. However, the existence of the texture became shorter as the concentration of the gelator increased. This is because the gelling rate was faster and the fingerprint texture of the cholesteric phase vanished as soon as the gelation occurred.

For comparison, the cooling process of bulk 5CB was observed using POM as well. As depicted in Fig. 4(d), only the schlieren texture was observed. This indicated that the addition of the cholesteric type gelator into 5CB induced a chiral nematic phase that was not observed in the bulk 5CB. This texture revealed that mesogenic molecules were oriented perpendicularly to glass substrate with the helical axis in plane with the cell during gelation. Finally, aggregation occurred in the chiral nematic medium. In contrast to a conventional gelator, gelation usually occurred in the isotropic state of the liquid crystal [16–23].

Variable-temperature infrared measurements were performed on the G1/5CB physical gel to investigate the gelling mechanism of G1. IR spectra were taken at 27, 40 and 60 °C, corresponding to the nematic gel, isotropic gel and isotropic state of the G1/5CB physical gel, respectively. Overall, all the peaks were retained except for C═O stretching. For the IR spectrum measured at 40 °C, the IR peaks became broader. The full width at half maximum (FWHM) increased from 13.3 cm^{-1} to 17.5 cm^{-1}. This indicated that the arrangement of molecules was more disordered at higher temperatures. After heating up to 60 °C, the G1/5CB physical gel melted and became an isotropic solution in which the gel networks had been destroyed. At this point, a drastic change was observed in the C═O stretching band, as shown in Fig. 5. The C═O stretching band became broader and the frequency shifted from 1736 to 1732 cm^{-1}. The FHWM became 27.0 cm^{-1}. The redshift was caused by the withdrawal of electron density from the adjacent C═O groups, since gelator molecules move freely in the isotropic state. In particular, there was an intermolecular interaction between carbonyl dipoles that brought the carbonyl groups closer and hence facilitated the formation of the gel at room temperature [24].

To best of our knowledge, gelation based on carbonyl-carbonyl interaction is not yet been reported. According to F.H. Allen, the carbonyl-carbonyl interaction could be comparable to medium-strength hydrogen bond, depending on the geometries of interactions which are sheared anti parallel, sheared parallel and perpendicular [25,26]. For example, carbonyl-carbonyl interaction has been proven to be able to stabilize the partially allowed conformations of asparagine and aspartic acid [27]. Besides, carbonyl-carbonyl interaction also involves in the self-assembly of several compounds such as ethyl N-(2-acetylphenyl)oxalamate, the supramolecular structure of ethyl 6-chloro-2-oxo-2H-chromene -3-carboxylate and ethyl 6-bromo-2-oxo-2H-chromene-3-carboxylate and the supramolecular structures of silver(I) complexes with 2,6-pyridinediylbis(4-pyridinyl)methanone [28–30]. All these evidences showed that carbonyl-carbonyl interaction is able to facilitate the self-assembly of the gelation.

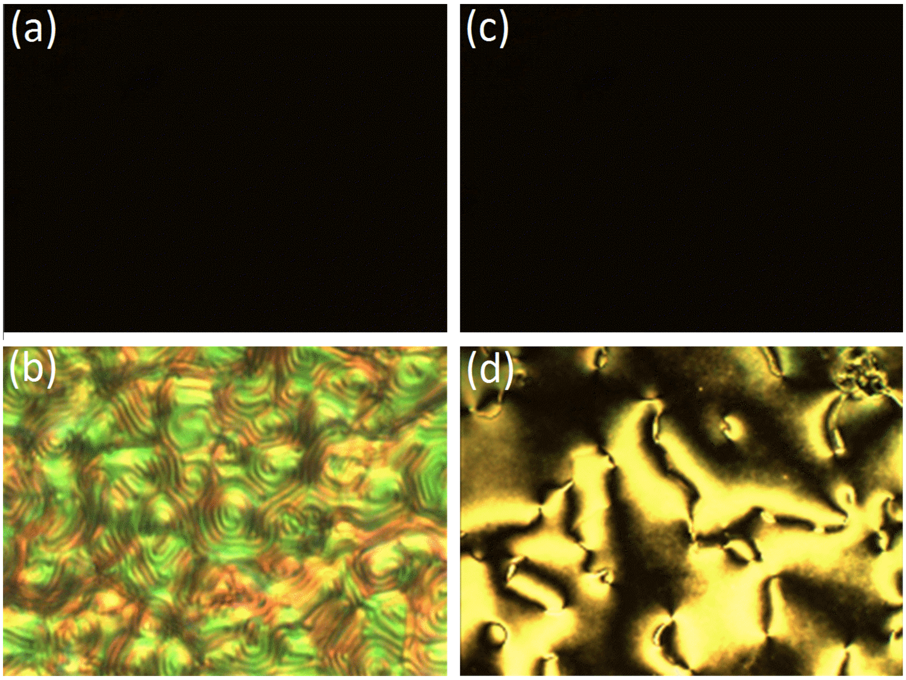

Fig. 4. Polarized optical micrographs of 6.0 wt% G1/5CB at (a) isotropic state, (b) chiral nematic state; bulk 5CB at (c) isotropic state and (d) nematic state.

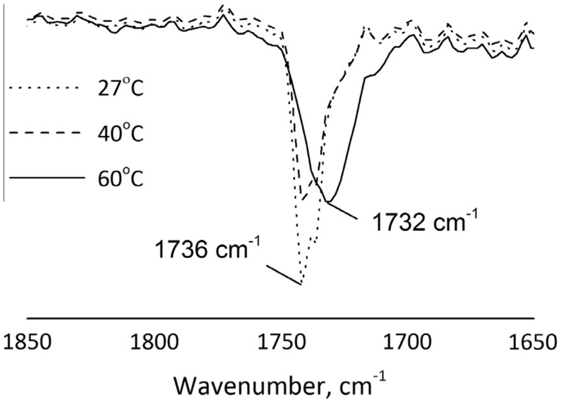

Fig. 5. Temperature-dependent IR spectra of 48.0 wt% G1/5CB in the region of 1650–1850 cm^{-1}.

3.2. Morphology study of liquid crystal physical gel

It was found that the macrophase-separated structure was highly dependent on the cooling conditions during gelation. G1/5CB of all compositions were observed using POM. The POM micrographs of 6.0, 12.0 and 24.0 wt% G1/5CB were provided in Supplementary Material 1. In this section, discussion is focused on 48.0 wt% G1/5CB since it possessed the most optimum electro-optical performance as shown in Section 3.4. Fig. 6(a) shows the POM images of 48.0 wt% G1/5CB prepared at room temperature, with a spherulite-like aggregation texture [31]. This texture is commonly observed in the crystallisation of high degree polymers such as nylon. The spherulites exhibited the typical Maltese black cross with arms parallel and perpendicular in the direction of the polarisers. The alignment of the gel aggregates was expected to be in the form of untwisted lamellae [32]. The growth mechanism of G1 confirmed that aggregation extended radially [33–35]. In contrast, 48.0 wt% G1/5CB prepared using rapid cooling showed a more homogeneous physical texture (Fig. 6(b)). Spherulite-like growth of gelation was not observed in this case. The POM results show that rapid cooling suppressed the growth of higher order structures such as spherulite-like aggregates [36]. Hence, a homogenous texture with finer gel aggregates was obtained, regardless of the concentration of the gelator.

In order to obtain more detailed insight into G1 aggregates, 5CB was extracted from the 48.0 wt% G1/5CB composite by immersing the sample in hexane:ethyl acetate (1:10) for 3 h. After drying, the

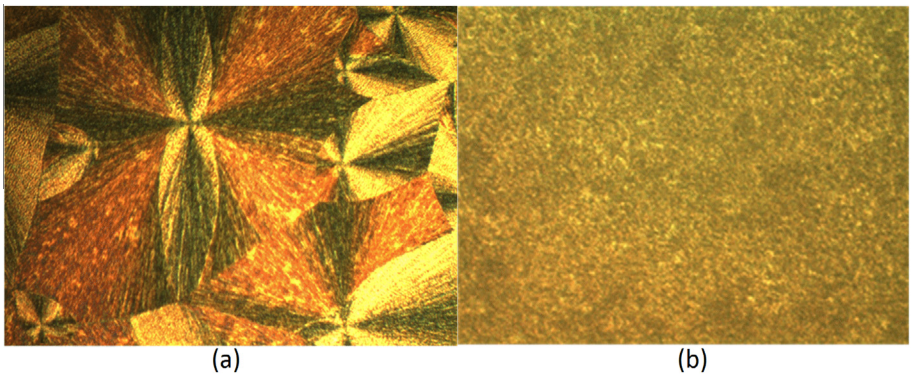

Fig. 6. Polarized optical micrographs of 48.0 wt% G1/5CB prepared at (a) room temperature and (b) rapid cooling.

resulting xerogel was observed using SEM. The xerogel formed with continuous cooling consisted of micron-sized pores of non-uniform shapes. As shown in Fig. 7(a) and (b), the micropores were mostly elongated in shape. This finding was compatible with the POM images of the spherulite-like aggregates that formed with continuous cooling. During gelation, spherulites impinged with each other, forming porous structure.

The possible molecular mechanism of aggregation is illustrated in Fig. 8. On the other hand, 48.0 wt% G1/5CB prepared with rapid cooling consisted of well-dispersed uniform spherical micropores of ca. 2 μm that were formed by the assembly of plate-like aggregates. Spherulite aggregations were not observed. Conventional gelators mostly produce fibrillar aggregates, where interconnected fibres form pores of random shapes [22,23,37,38]. The spherical-type pore shape formed by a liquid crystal physical gel is rarely reported.

3.3. Liquid crystal director orientation in liquid crystal physical gel

ESR spectroscopy was employed to study the liquid crystal director distribution in different macrophase-separated structures. Since both 5CB and G1 are diamagnetic, the 3β-doxyl-5α-cholestane free radical was added as a spin probe. This free radical has a rod-like structure, resulting in a strong interaction with the 5CB host. Fig. 9 shows the ESR spectrum of the 3β-doxyl-5α-cholestane free radical in nematic 5CB. The ESR spectrum consisted of three characteristic spectral lines because of the hyperfine splitting effect between the unpaired electron from the N—O group in 3β-doxyl-5α-cholestane with the nuclear spin of the ^{14}N nucleus. Spectral lines were slightly broadened and showed unequal intensities. This was caused by incomplete motional averaging of the hyperfine tensor and g tensor in the viscous medium 5CB. Without any disturbant, the spin probe was localised in a uniform medium

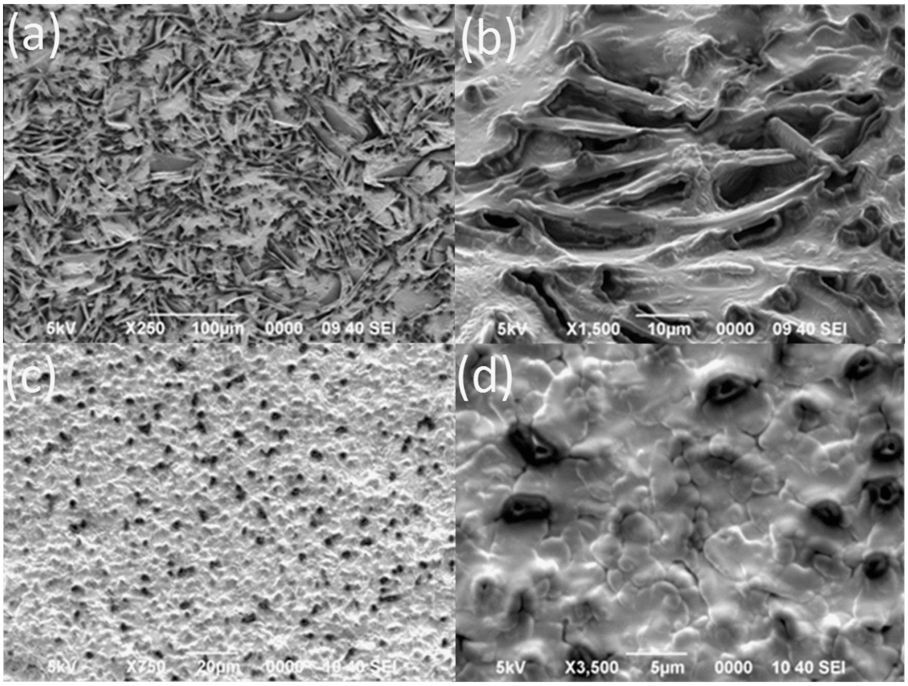

Fig. 7. SEM micrographs of 48.0 wt% G1/5CB prepared at room temperature observed at (a) 250 magnification and (b) 1500 magnification; prepared in rapid cooling observed at (c) 750 magnification and (d) 3500 magnification.

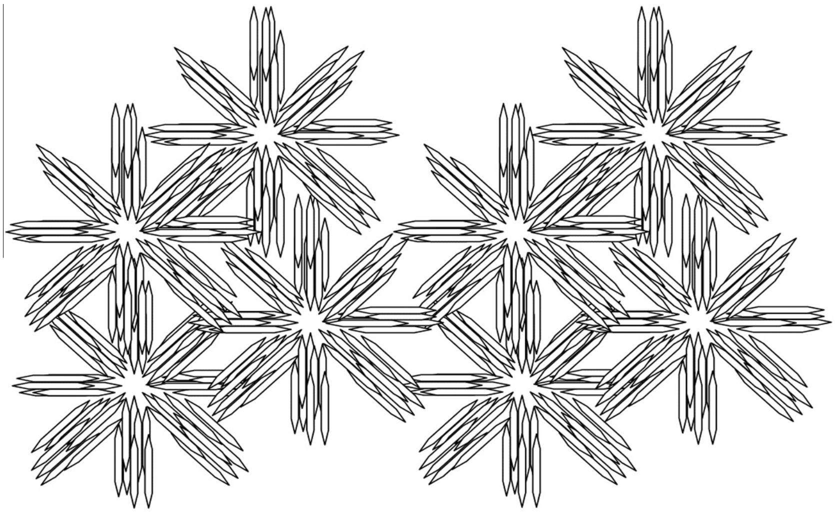

Fig. 8. Illustration on the pore forming by spherulite-like aggregations.

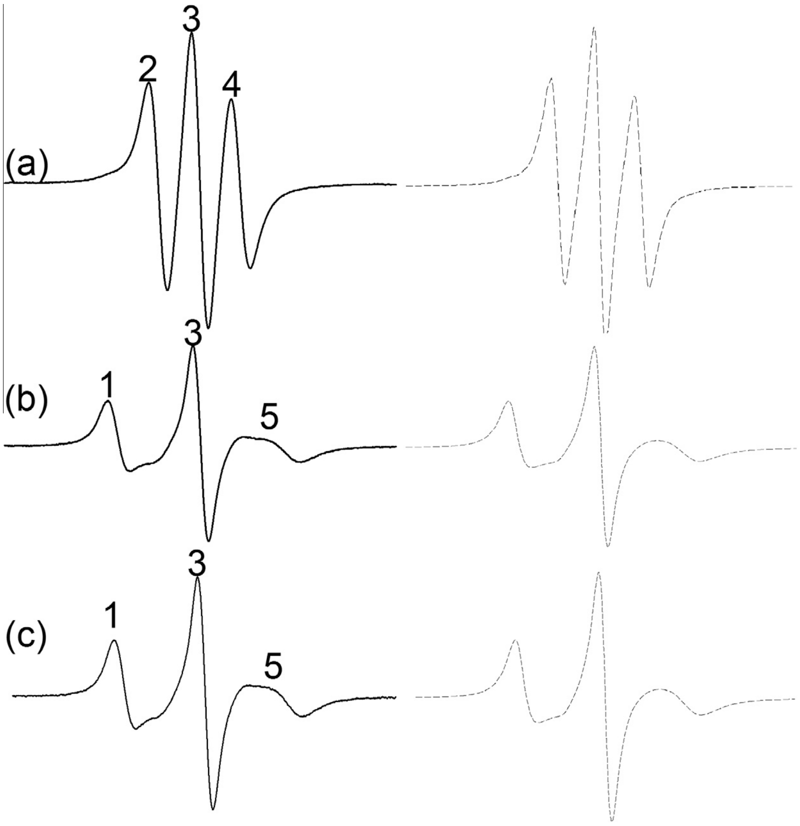

Fig. 9. ESR spectra of (a) 5CB and (b) 48.0 wt% G1/5CB formed under rapid cooling and (c) 48.0 wt% G1/5CB formed at room temperature. Dash lines are simulated spectra.

of 5CB that was aligned parallel to the magnetic field due to its positive magnetic anisotropy. Hyperfine spacing was measured as 0.87 mT. This spectrum is a guideline to determine the existence of an aligned director in a liquid crystal physical gels. The ESR spectra of 48.0 wt% G1/5CB prepared under both cooling conditions were obtained in powder form. These spectra consisted of five peaks instead of the three observed in the bulk 5CB. Apparently, peak 2 and 4 had been massively distorted. Conversely, peak 1 arose at the lower field, about 1.79 mT from the centre peak. This indicated that most of the liquid crystal directors had been massively randomised when gel networks existed in the medium. Under such conditions, most of the 5CB molecules were expected to be entangled close to the fibrous networks. The director orientational order was further confirmed by a spectral simulation derived from the torque-balanced equation [39,40]. The second rank order parameter was found to be unity for 48.0 wt% G1/5CB under both cooling conditions, indicating the director orientational order had been broken down. The existence of randomised liquid crystal directors in micron-size domains is predicted to generate a strong light scattering effect and could be useful for electro-optical applications. The electro-optical performance is discussed in the following section.

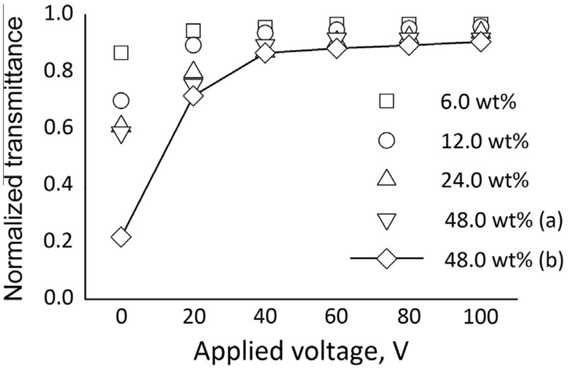

Fig. 10. Relationship between light transmittance and applied voltage of liquid crystal physical gels.

3.4. Electro-optical behaviour of liquid crystal physical gel

A random director orientation in a macrophase-separated structure is actually beneficial for light scattering electro-optical displays. The light scattering behaviour of G1/5CB physical gels was examined, as shown in Fig. 10. In the off-stage, a light scattering effect was induced by the mismatch of the refractive indices of the liquid crystal and the gel network. When current was applied to the cell, the 5CB molecules were reoriented to produce a transparent state. Light scattering behaviour was found to be dependent on the morphologies of the physical gel. In the off-stage, light transmittance was reduced as the concentration of the gelator was increased. As shown by ESR, the second rank order parameter was unity when the concentration of the gelator was increased above 6.0 wt%. The light scattering effect was again strongly affected by the macrophase-separated structure. As the gelator concentration increased, thicker aggregates assembled to form smaller pores. The 48.0 wt% G1/5CB physical gels consisted of micron-sized pores and therefore the light scattering effect was enhanced. As shown in Fig. 10, 48.0 wt% G1/5CB prepared with rapid cooling had the highest light transmittance contrast ratio, 4.2.

The liquid crystal gels visually showed clear switching between the turbid and transparent states, as shown in Fig. 11. It is thought that the light scattering effect was induced by the well-dispersed

Table 1
Comparison of liquid crystal physical gels for light scattering performance.

Liquid crystal physical gels	Gelation bonding	Gel structure	Pore shape	Contrast ratio	V_{10}–V_{90}	Rise time/decay time (µs)	Ref.
G1/5CB	Carbonyl-carbonyl interaction	Plate-shaped	Spherical (2 µm)	4.2	5–29 V	3.7/22,500	This study
GA/5CB	Hydrogen bonding	Fibrillar	Random (1–2 µm)	67	10–37 V	500/1800	[22]
ZI18/5CB	Hydrogen bonding	Fibrillar	Random (10 µm)	7	6–86 V	500/1000	[23]
N,N′-Distearoyl-3,3′-dimethyl-4,4′-diaminodiphenylmethane/5CB	Hydrogen bonding	Fibrillar	Random	–	–	–	[37]
DMDBS/5CB	Hydrogen bonding	Fibrillar	Random (70 µm)	8.7	3–30 V	1500/38,500	[38]

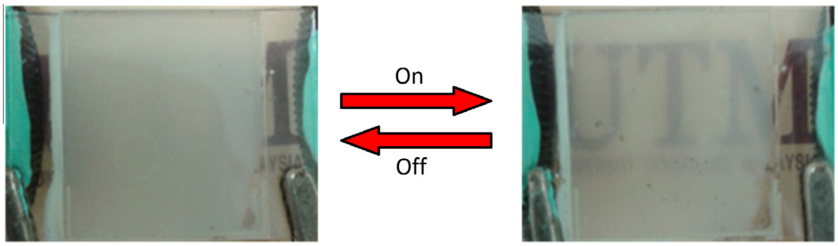

Fig. 11. Electro-optical switching between light scattering and transparent state.

uniform spherical micropores with a homogenous texture. Additionally, the pore size is comparable to the wavelength of visible light. The contrast ratio was considered low as compared to the conventional gelator, as shown in Table 1. For improvement, the difference in the refractive indices of 5CB and gelator should be increased. Besides the contrast ratio, the driving voltage and response time are important factors for light scattering displays. In general, these two factors are greatly dependent on the surface anchoring force between liquid crystal domains and the interfacial area close to the gel network. As shown in Table 1, G1/5CB had the lowest threshold voltage and fastest response time of 5.0 V and 3.7 µs, respectively. This indicates that the surface anchoring force of the G1 gel network was weak, although it was still sufficient to generate a randomised director orientation in the liquid crystal domains. This trait has great potential for highly responsive electro-optical applications. However, the decay time was comparatively high. This is because the decay time can only be shortened in the presence of a strong anchoring force that encourages the molecules to relax back into their original position when the electric field is removed.

Table 1 shows the comparison of G1/5CB with conventional liquid crystal physical gels applied for light scattering displays. It clearly shows that most of the reported gelators produce fibrillar gel networks as induced by the unidirectional self-assembly of hydrogen bonding. On the contrary, G1/5CB showed a unique gel structure consisting of spherical micropores. This structure was formed by the carbonyl-carbonyl interaction in G1 under liquid nitrogen rapid cooling. Combining the electro-optical performance and the gel structure, it was found that spherical micropores produced by cholesteric type G1 were beneficial to the light scattering effect. To the best of our knowledge, the preparation of a liquid crystal physical gel using a mesogenic type gelator is rare, and worth exploring further due to its flexibility for tailoring the alignment of gel networks.

4. Conclusions

A liquid crystal physical gel has been developed as a material for light scattering display [4,5]. The self-assembly of the chiral gelator, cholesteryl stearate in 4-cyano-4′-pentylbiphenyl nematic liquid crystal facilitates the formation of the macrophase-separated structure that is applicable to the light scattering systems. The chirality of the gelator induces chiral nematic phase during gelation and hence plate-like aggregates are formed. These plate-like aggregates effectively form uniform spherical micropores instead of random structures compared to the fibrous gel network of conventional gelator [22,23,37,38]. Theoretically, different gel morphology possesses different electro-optical properties [23,36]. For this liquid crystal physical gel, the electro-optical performance is not only comparable to the reported systems, but even with improved response time in microsecond. The light scattering effect is attributed to the well-distributed spherical pores that consisting of a liquid crystal with a random director.

It is interesting to note that the chiral gelator could form a gel network of different morphology compared to the conventional non-mesogenic gelator, perhaps suggesting the potential of mesogenic gelator in producing the liquid crystal physical gel. This study is useful for future study of preparation of the liquid crystal physical gel using mesogenic gelator. Significantly, it may contribute to the understanding of the preparation of physical gel in the nanoscale.

Acknowledgement

This work is supported by the Malaysian Ministry of Higher Education (MOHE) via Exploratory Research Grant Scheme (Vot No. 4L120) and MyPhD Scholarship (Leaw Wai Loon).

Appendix A. Supplementary material

Supplementary data associated with this article can be found, in the online version, at http://dx.doi.org/10.1016/j.jcis.2016.08.020.

References

[1] G. Mathew, Synthesis and Characterization of Hydrogel Polymers, first ed., Auris Reference Limited, 2014.
[2] D. Coates, Polymer-dispersed liquid crystals, J. Mater. Chem. 5 (12) (1995) 2063–2072.
[3] S. Bronnikov, S. Kostromin, V. Zuev, Polymer-dispersed liquid crystals: progress in preparation, investigation, and application, J. Macromol. Sci., Part B 52 (12) (2013) 1718–1735.
[4] T. Kato, Y. Hirai, S. Nakaso, M. Moriyama, Liquid-crystalline physical gels, Chem. Soc. Rev. 36 (12) (2007) 1857–1867.

[5] T. Kato, N. Mizoshita, M. Moriyama, T. Kitamura, Gelation of Liquid Crystals With Self-Assembled Fibers, Low Molecular Mass Gelator, Springer, Berlin Heidelberg, 2005, pp. 219–236.
[6] S.R. Raghavan, B.H. Cipriano, Gel formation: phase diagrams using tabletop rheology and calorimetry, in: R.G. Weiss, P. Terech (Eds.), Molecular Gels: Materials With Self-Assembled Fibrillar Networks, Springer, Netherlands, Dordrecht, 2006, pp. 241–252.
[7] J. Prigann, C. Tolksdorf, H. Skupin, R. Zentel, F. Kremer, FT-IR spectroscopic studies on reorientation of ferroelectric liquid crystals in a thermoreversible gel network, Macromolecules 35 (10) (2002) 4150–4154.
[8] M. Andreis, D. Carić, N.Š. Vujičić, M. Jokić, M. Žinić, M. Kveder, Self-assembly of gelator molecules in liquid crystals studied by ESR, Chem. Phys. 403 (2012) 81–88.
[9] P.H. Rieger, R.S.o. Chemistry, Electron Spin Resonance: Analysis and Interpretation, RCS (Royal Soc. of Chemistry) Publ., 2007.
[10] G. Jeschke, S. Schlick, Continuous-Wave and Pulsed ESR Methods, Advanced ESR Methods in Polymer Research, John Wiley & Sons, Inc., 2006, pp. 1–24.
[11] I. Gnatyuk, G. Puchkovskaya, O. Yaroshchuk, Y. Goltsov, L. Matkovskaya, J. Baran, T. Morawska-Kowal, H. Ratajczak, Spectroscopic study of liquid crystals in confined volume, J. Mol. Struct. 511–512 (1999) 189–197.
[12] G. Wang, X.L. Zhao, Y. Zhao, Synthesis of azobenzene-containing liquid crystalline gelator for use in liquid crystal gels, Chin. Chem. Lett. 19 (5) (2008) 521–524.
[13] X. Wang, Q. Zhou, Liquid Crystalline Polymers, World Scientific Publishing Company, 2004.
[14] P.J. Collings, M. Hird, Introduction to Liquid Crystals: Chemistry and Physics, CRC Press, 1997.
[15] J.W. Goodby, Introduction to defect textures in liquid crystals, in: J. Chen, W. Cranton, M. Fihn (Eds.), Handbook of Visual Display Technology, Springer, Berlin Heidelberg, Berlin, Heidelberg, 2012, pp. 1289–1314.
[16] T. Kato, T. Kutsuna, K. Hanabusa, M. Ukon, Gelation of room-temperature liquid crystals by the association of a trans-1,2-bis(amino)cyclohexane derivative, Adv. Mater. 10 (8) (1998) 606–608.
[17] T. Kato, T. Kutsuna, K. Hanabusa, Liquid-crystalline physical gels formed by the aggregation of trans-(1R,2R)-bis(dodecanoylamino)cyclohexane in a thermotropic nematic liquid crystal. phase behavior and electro-optic properties, Mol. Cryst. Liquid Cryst. Sci. Technol.. Section A. Mol. Cryst. Liquid Cryst. 332 (1) (1999) 377–382.
[18] K. Yabuuchi, A.E. Rowan, R.J.M. Nolte, T. Kato, Liquid-crystalline physical gels: self-aggregation of a gluconamide derivative in mesogenic molecules for the formation of anisotropic functional composites, Chem. Mater. 12 (2) (2000) 440–443.
[19] N. Mizoshita, K. Hanabusa, T. Kato, Nematic liquid-crystalline physical gels exhibiting faster responses to electric fields in twisted nematic cells, Displays 22 (1) (2001) 33–37.
[20] N. Mizoshita, K. Hanabusa, T. Kato, Self-aggregation of an amino acid derivative in a liquid-crystalline physical gel—faster response to electric fields, Adv. Mater. 11 (5) (1999) 392–394.
[21] N. Mizoshita, T. Kutsuna, K. Hanabusa, T. Kato, Physical gelation of nematic liquid crystals with amino acid derivatives leading to the formation of soft solids responsive to electric field, J. Photopolym. Sci. Technol. 13 (2) (2000) 307–312.
[22] N. Mizoshita, Y. Suzuki, K. Kishimoto, K. Hanabusa, T. Kato, Electrooptical properties of liquid-crystalline physical gels: a new oligo(amino acid) gelator for light scattering display materials, J. Mater. Chem. 12 (8) (2002) 2197–2201.
[23] N. Mizoshita, Y. Suzuki, K. Kishimoto, T. Kato, K. Hanabusa, Light scattering electrooptic behavior of liquid-crystalline physical gels — effects of microphase-separated morphologies, Mol. Cryst. Liq. Cryst. 409 (1) (2004) 175–181.
[24] Y. Mazur, F. Sondheimer, 1,4-Carbonyl-carbonyl interactions, Experientia 16 (5) (1960) 181–184.
[25] F.H. Allen, C.A. Baalham, J.P.M. Lommerse, P.R. Raithby, Carbonyl-carbonyl interactions can be competitive with hydrogen bonds, Acta Crystallogr. Section B-Struct. Sci. 54 (3) (1998) 320–329.
[26] A. Gavezzotti, Packing analysis of organic crystals containing carbonyl or cyano groups, J. Phys. Chem. 94 (10) (1990) 4319–4325.
[27] C.M. Deane, F.H. Allen, R. Taylor, T.L. Blundell, Carbonyl-carbonyl interactions stabilize the partially allowed Ramachandran conformations of asparagine and aspartic acid, Protein Eng. 12 (12) (1999) 1025–1028.
[28] L.C. Cabrera-Pérez, E.V. García-Báez, M.O. Franco-Hernández, F.J. Martínez-Martínez, I.I. Padilla-Martínez, Carbonyl-carbonyl interactions and amide π-stacking as the directing motifs of the supramolecular assembly of ethyl N-(2-acetylphenyl)oxalamate in a synperiplanar conformation, Acta Crystallogr. Section C 71 (5) (2015) 381–385.
[29] R.J. Santos-Contreras, F.J. Martínez-Martínez, E.V. García-Báez, I.I. Padilla-Martínez, A.L. Peraza, H. Höpfl, Carbonyl-carbonyl, carbonyl–π and carbonyl-halogen dipolar interactions as the directing motifs of the supramolecular structure of ethyl 6-chloro-2-oxo-2h-chromene-3-carboxyl-ate and ethyl 6-bromo-2-oxo-2h-chromene-3-carboxyl-ate, Acta Crystallogr. Section C 63 (4) (2007) o239–o242.
[30] C.-Q. Wan, T.C.W. Mak, Unusual carbonyl···carbonyl interaction in supramolecular structures of Silver(I) complexes with 2,6-pyridinediylbis(4-pyridinyl)methanone, Cryst. Growth Des. 11 (3) (2011) 832–842.
[31] H. Abe, H. Kikuchi, T. Kajiyama, K. Hanabusa, T. Kato, Morphological studies of a (self-assembling oil gelator/liquid crystal) composite system, Liq. Cryst. 29 (12) (2002) 1503–1508.
[32] M. Goel, M. Jayakannan, Supramolecular liquid crystalline π-conjugates: the role of aromatic π-stacking and van der Waals Forces on the molecular self-assembly of oligophenylenevinylenes, J. Phys. Chem. B 114 (39) (2010) 12508–12519.
[33] A. Keller, The morphology of crystalline polymers, Die Makromol. Chem. 34 (1) (1959) 1–28.
[34] J.H. Magill, Spherulitic crystallization. Part I. "Odd-Even" polyamides: Nylon 56 and Nylon 96, J. Polym. Sci. Part A: Gen. Pap. 3 (3) (1965) 1195–1219.
[35] F.P. Price, The structure of high polymer spherulites, J. Polym. Sci. 37 (131) (1959) 71–89.
[36] H. Abe, H. Kikuchi, K. Hanabusa, T. Kato, T. Kajiyama, Morphology control of liquid crystalline composite gels based on molecular self-assembling kinetics, Liq. Cryst. 30 (12) (2003) 1423–1431.
[37] J. He, B. Yan, B. Yu, R. Bao, X. Wang, Y. Wang, Effect of the structure of gelators on electro-optical properties of liquid crystal physical gels, J. Colloid Interface Sci. 316 (2) (2007) 825–830.
[38] S. Bi, H. Peng, S. Long, M. Ni, Y. Liao, Y. Yang, Z. Xue, X. Xie, High modulus and low-voltage driving nematic liquid-crystalline physical gels for light-scattering displays, Soft Matter 9 (32) (2013) 7718–7725.
[39] G.R. Luckhurst, On the creation of director disorder in nematic liquid crystals, Thin Solid Films 509 (1–2) (2006) 36–48.
[40] F.M. Leslie, G.R. Luckhurst, H.J. Smith, Magnetohydrodynamic effects in the nematic mesophase, Chem. Phys. Lett. 13 (4) (1972) 368–371.